

Coupling a 1D Dual-permeability Model with an Infinite Slope Stability Approach to Quantify the Influence of Preferential Flow on Slope Stability

Shao, Wei; Bogaard, Thom; Su, Ye; Bakker, Mark

DOI

[10.1016/j.proeps.2016.10.014](https://doi.org/10.1016/j.proeps.2016.10.014)

Publication date

2016

Document Version

Final published version

Published in

Procedia: Earth and Planetary Science

Citation (APA)

Shao, W., Bogaard, T., Su, Y., & Bakker, M. (2016). Coupling a 1D Dual-permeability Model with an Infinite Slope Stability Approach to Quantify the Influence of Preferential Flow on Slope Stability. *Procedia: Earth and Planetary Science*, 16, 128-136. <https://doi.org/10.1016/j.proeps.2016.10.014>

Important note

To cite this publication, please use the final published version (if applicable). Please check the document version above.

Copyright

Other than for strictly personal use, it is not permitted to download, forward or distribute the text or part of it, without the consent of the author(s) and/or copyright holder(s), unless the work is under an open content license such as Creative Commons.

Takedown policy

Please contact us and provide details if you believe this document breaches copyrights. We will remove access to the work immediately and investigate your claim.

The Fourth Italian Workshop on Landslides

Coupling a 1D dual-permeability model with an infinite slope stability approach to quantify the influence of preferential flow on slope stability

WeiShao^{a*}, Thom Bogaard^a, YeSu^b, Mark Bakker^a

^a *Water Resources Section, Faculty of Civil Engineering and Geosciences, Delft University of Technology, 2628CN, Delft, Netherlands*

^b *Department of Physical Geography and Geoecology, Faculty of Science, Charles University in Prague, 12843, Prague, Czech Republic*

Abstract

In this study, a 1D hydro-mechanical model was developed by coupling a dual-permeability model with an infinite slope stability approach to investigate the influence of preferential flow on pressure propagation and slope stability. The dual-permeability model used two modified Darcy-Richards equations to simultaneously simulate the matrix flow and preferential flow in a slope. The simulated pressure head was sequentially coupled with the soil mechanics model. The newly-developed numerical model was codified with the Python programming language, and benchmarked against the HYDRUS-1D software. The benchmark example showed that the proposed model is able to simulate the non-equilibrium phenomenon in a heterogeneous soil. We further implemented the model to conduct a synthetic experiment designing a slope with heterogeneous soil overlying an impermeable bedrock as a combined analysis of hydrology and slope stability, the results shows that the occurrence of preferential flow can reducing the time and rainfall amount required for slope failure. The proposed model provides a relatively simple and straightforward way to quantify the effect of preferential flow on the pressure propagation and landslide-triggering in heterogeneous hillslope.

© 2016 The Authors. Published by Elsevier B.V. This is an open access article under the CC BY-NC-ND license (<http://creativecommons.org/licenses/by-nc-nd/4.0/>).

Peer-review under responsibility of the organizing committee of IWL 2015

Keywords: preferential flow; dual-permeability model; infinite slope stability approach; pressure propagation

* Corresponding author. Tel.: 31(0)684331920; fax: +31(0)152781029.
E-mail address: W.SHAO@TUDELFT.NL

1. Introduction

Rainfall-induced shallow landslides are among one of the most frequent natural hazards in mountainous areas¹⁻³. Slope instability is often initiated by a fast pore-water pressure response to precipitation or snow-melt events that reduces the suction stress and shear strength of the slope³⁻⁴. Therefore, quantification of pore pressure propagation in a subsurface hydrological system is critical to simulate the timing and location of rainfall-triggered landslides⁴⁻⁶.

In response to rain-pulses, the pressure propagation in a saturated soil is nearly-instant due to a low compressibility of the saturated soil⁵⁻⁶. While, in an unsaturated soil, fast pore water response might be related with preferential flow bypassing the adjacent soil matrix, directly reaching the groundwater table⁷⁻¹⁰. Preferential flow paths, such as cracks, macropores, fissures, pipes, etc., are common features in slopes⁶⁻¹¹. Increasingly sophisticated models have been developed for simulating preferential flow in various environmental systems¹²⁻¹⁴. The widely-used dual-permeability models conceptualize the soil as two porous domains that interact hydrologically: the more permeable domain with associated larger porosity represents the macropores, fractures, fissures, and cracks; and the less permeable domain with lower porosity represents the soil matrix¹⁴⁻¹⁷.

Yet, most of the hydro-mechanical models calculate the pore water pressure based on a single-permeability assumption¹⁸, and the effects of preferential flow on pressure wave propagation and landslide-triggering under high-intensity rainstorms are rarely quantified. Therefore, the objective of this paper is to describe a hydro-mechanical model, which couples a 1D dual-permeability model simulating infiltration and lateral flow along a slope gradient with an infinite slope stability approach. Such direct coupling of dual-permeability hillslope hydrological model and slope stability calculation allows to quantify the influence of preferential flow on slope stability under different boundary conditions. First we present the model set up, then we use a synthetic numerical experiment for model validation. Thereafter, we investigate pressure propagation and landslide-triggering under the influence of preferential flow in a pre-defined heterogeneous hillslope.

2. Model description and numerical implementation

2.1. Steady initial pressure distribution

In a conceptualized 2D hillslope, the groundwater table at lower part of the slope is higher, which is therefore highly correlated with the slope failure. Here, we adopt a widely-used approach to estimate the groundwater table at the lower part of the slope that further can assist in specifying an initial pressure distribution along a vertical profile of the slope. Considering a long-term lateral steady flow parallel to the slope (Fig.1), the water table height at the slope bottom h_G can be expressed as³:

$$h_G = \frac{L(R-E) - Q_{leak}}{K \sin \alpha} \quad (1)$$

Where α (deg) is the slope angle, K (LT^{-1}) is the hydraulic conductivity of the soil material, L (L) is the length of a slope, R and E (LT^{-1}) are the flow rate of rainfall and evaporation, and Q_{leak} (L^2T^{-1}) is the groundwater leakage.

Assuming a leakage flow q_{leak} (LT^{-1}) normal to the bottom boundary of the slope, the specific discharge q in the normal direction (Z) of the slope can be expressed by Darcy's Law⁵:

$$q(Z)|_{Z < h_G} = -K_s \left(\frac{\partial h}{\partial Z} + \cos \alpha \right) = -q_{leak} \quad (2)$$

where h (L) is the pressure head, K_s (LT^{-1}) is the saturated hydraulic conductivity. Equation (2) implies that an extra elevation head of gravitational gradient ($\sin \alpha$ in Eq.1) drives a parallel saturated flow in the hillslope ($\cos \alpha$ in Eq.2). As a result, the water pressure head distribution can be derived as:

$$h(Z)|_{Z < d_G} = (d_G - Z) \left[\cos \alpha - \frac{q_{leak}}{K_s} \right] \quad (3)$$

Furthermore, the pressure distribution at a vertical coordinate system can be written as:

$$h(z)|_{z < h_G} = (h_G - z) \left[\cos^2 \alpha - \frac{q_{leak}}{K_s} \cos \alpha \right] \quad (4)$$

where $z(L)$ is the vertical coordinate (positive upward).

For hydrostatic conditions, the initial pressure head distribution can approximately be specified with a linear distribution following Eq.4 for the vertical soil profile.

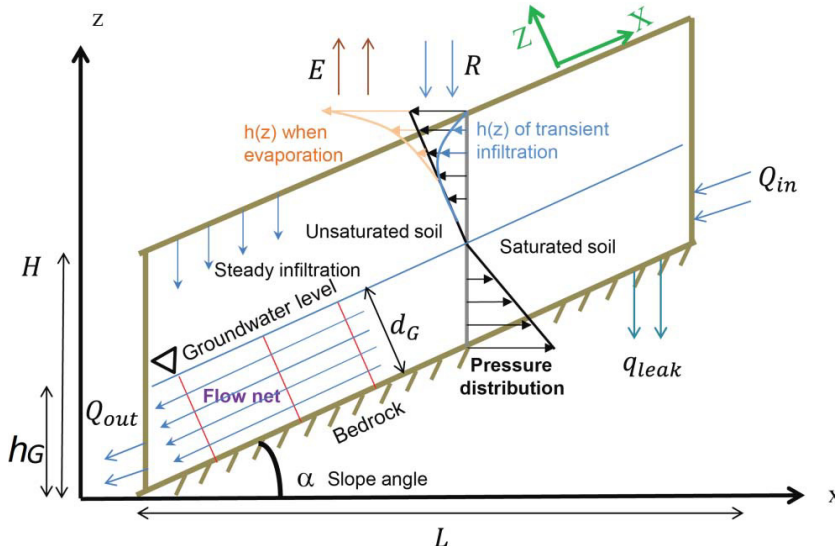


Fig.1 Schematic of the slope with a plane geometry

2.2. Transient pressure response

In a hillslope, the transient pressure response to rain-pulses can be simulated by the modified Darcy-Richards equation that was originally proposed as a single-permeability model¹⁹. Here we extend it to a modified dual-permeability model to simulate matrix flow as well as preferential flow¹⁵:

$$\begin{cases} C_f \frac{\partial h_f}{\partial t} = \frac{\partial}{\partial z} \left[K_f \left(\frac{1}{\cos^2 \alpha} \frac{\partial h_f}{\partial z} + 1 \right) \right] - \frac{\Gamma_w}{w_f} \\ C_m \frac{\partial h_m}{\partial t} = \frac{\partial}{\partial z} \left[K_m \left(\frac{1}{\cos^2 \alpha} \frac{\partial h_m}{\partial z} + 1 \right) \right] + \frac{\Gamma_w}{w_m} \\ \Gamma_w = \alpha_w \frac{K_m(h_f) + K_m(h_m)}{2} (h_f - h_m) \end{cases} \quad (5)$$

where the subscript f indicates the preferential flow domain, the subscript m indicates the matrix domain, t (T) is time, θ ($L^3 L^{-3}$) is the water content, C ($d\theta/dh$) (L^{-1}) is the differential water capacity, h (L) is the pressure head, K (LT^{-1}) is the unsaturated hydraulic conductivity, w (-) is the volume fraction of the preferential flow domain or the matrix domain, Γ_w (T^{-1}) is the water exchange term, and α_w (L^{-2}) is the water exchange coefficient¹⁹.

The Mualem-van Genuchten model is used to describe the hydraulic properties of both the matrix and the preferential flow domains²⁰:

$$\Theta = \frac{\theta - \theta_r}{\theta_s - \theta_r} = \begin{cases} \left[1 + |\alpha_{\text{VG}} h|^{n_{\text{VG}}} \right]^{-m_{\text{VG}}}, & h < 0 \\ 1, & h \geq 0 \end{cases} \quad (6)$$

$$C(\Theta) = \begin{cases} m_{\text{VG}} n_{\text{VG}} \alpha_{\text{VG}} (\theta_s - \theta_r) \Theta^{1/m_{\text{VG}}} (1 - \Theta^{1/m_{\text{VG}}})^{m_{\text{VG}}}, & h < 0 \\ S_s, & h \geq 0 \end{cases} \quad (7)$$

$$K(\Theta) = K_s \Theta^{0.5} \left[1 - (1 - \Theta^{1/m_{\text{VG}}})^{m_{\text{VG}}} \right]^2 \quad (8)$$

where $\Theta(-)$ is the effective saturation; $\theta(\text{L}^3\text{L}^{-3})$ is the volumetric water content with subscript r and s denote the residual and saturated state; $\alpha_{\text{VG}}(\text{L}^{-1})$, $n_{\text{VG}}(-)$, and $m_{\text{VG}}(-)$ are fitting parameters; $S_s(\text{L}^{-1})$ denotes the specific storage.

2.3. Surface boundary condition for dual-permeability model

The boundary conditions of the Darcy-Richards equation could be specified for pressure head, flux, or mixed¹⁶⁻¹⁷. The specified infiltration flux $i(\text{LT}^{-1})$ on a dual-permeability soil surface is divided into the two constituting domains:

$$i = w_f i_f + w_m i_m \quad (9)$$

where i_f and i_m are specified boundary fluxes on the surface of the matrix domain and the preferential flow domains respectively.

We assume the preferential flow not to be triggered at the beginning of a rainfall event, and consequently, the infiltration process starts in the matrix domain only:

$$R = i = w_m i_m \quad (10)$$

In case the specified flow at the matrix surface exceeds its infiltration capacity, the boundary condition of the matrix domain changes to a specified pressure head. Hereafter, the infiltration-excess water at that time-step will be reallocated to the surface boundary of preferential flow domain:

$$i_f = \frac{R - w_m i_m}{w_f} \quad (11)$$

Once the specified flux into the preferential flow domain is larger than its infiltration capacity, the boundary conditions of both domains are changed to the specified pressure head corresponding to the surface water ponding depth.

2.4. Infinite slope stability approach

Using an infinite slope stability approach to formulate the factor of safety $F_s(-)$, it is expressed as a ratio of resisting force to gravitationally driving force with three terms (i.e., friction angle term, cohesion term, and suction stress term)²¹:

$$F_s(z_H) = \frac{\tan \phi'}{\tan \alpha} + \frac{c'}{G \sin \alpha \cos \alpha} - \frac{\sigma^s}{G} \frac{\tan \phi'}{\sin \alpha \cos \alpha} \quad (12)$$

$$G = \int_{z_H}^H [\gamma_s + \gamma_w \theta] dz \quad (13)$$

$$\sigma^s = \chi p_w = \chi \gamma_w h \quad (14)$$

where $z_H(L)$ is the depth that below the soil surface; $c'(ML^{-2}T^{-2})$ is the effective cohesion; ϕ' (deg) is the friction angle; $G(ML^{-2}T^{-2})$ is the weight of soil; $\sigma^s(ML^{-2}T^{-2})$ is the suction stress; $p_w(ML^{-2}T^{-2})$ is the pore water pressure; and $\chi(-)$ is the matrix suction coefficient, which can be approximated by the effective saturation²².

2.5. Numerical implementation

The dual-permeability model is numerically solved by an author-developed script under Python2.7 programming environment, in which the algorithms use implicit finite difference method and Picard iteration technique in each time step²². During simulation, the tolerable error of water content is set to 0.0001, and the time step is dynamic in the range of 0.015~2 min, ensuring the numerical accuracy and computational efficiency.

The hydrological results are sequentially coupled with the soil mechanical calculations as follows: i) the soil moisture distribution (Eq.13) determines the unit self-weight of soil; ii) the effective saturation and the pore water pressure (Eq.14) influence the suction stress and consequently the shear strength. The dual-permeability model simulates the non-equilibrium phenomenon of different water contents, pore water pressures, and flow velocities between the two domains¹³⁻¹⁴. The total water content and effective saturation can be evaluated by the weighted average of two domains. In this study, the pore water pressure in the preferential flow domain is assumed to be the "effective pressure head" for calculating the slope stability analysis¹⁶⁻¹⁷. However, in Section 4 we show and discuss the differences of simulated slope stability using the pressure head from either the matrix domain or preferential flow domain.

3. Benchmark with HYDRUS-1D

A simple synthetic dual-permeability problem that can be simulated with HYDRUS-1D, is used as a benchmark case to demonstrate the ability, accuracy and effectiveness of our hydrological code for modelling non-equilibrium flow in a dual-permeability soil. We use a 10 hours constant-head infiltration experiment in a sandy-loam soil column with an infinitely-deep groundwater level. The soil is conceptualized with two domains, in which the preferential flow and matrix flow co-exist. First, the initial condition of dual-permeability model is specified with a unit hydraulic gradient of a uniform pore water pressure distribution with a value of -2 m H₂O in both the matrix domain and the preferential flow domain. Second, the specified upper boundary is a constant pressure head of -0.001 m H₂O, and the specified lower boundary is gravitational drainage. The parameters of two water retention curves and two soil hydraulic conductivity functions of the Mualem-van Genuchten model are specified in Table 1 following the approach of Kohne et al.²⁴. Lastly, the water exchange coefficient α_w is set to as a moderate value of 0.01 cm⁻² to be able to obtain a non-equilibrium phenomenon with a clear difference in water exchange between 2 domains.

Table 1 Soil hydraulic parameters for the dual-permeability model in Experiment 1

Sandy loam (depth:1m)	$w(-)$	$\theta_l(\text{cm}^3/\text{cm}^3)$	$\theta_s(\text{cm}^3/\text{cm}^3)$	$K_s(\text{cm}/\text{day})$	$\alpha_{VG}(\text{cm}^{-1})$	$n_{VG}(-)$	$l_{VG}(-)$	$\alpha_w(\text{cm}^{-2})$
Matrix domain	0.9	0.0	0.446	2.78	0.008	1.485	0.5	0.001
Preferential flow domain	0.1	0.0	0.76	296	0.188	1.269	0.5	

Fig.2 shows the infiltration development in 2-hour timestep profiles of simulated water content, pressure head, and water exchange fluxes in two domains. Fig. 2c shows the total water content as a weighted average, and Fig. 2f shows the water exchange between two domains. Under a surface ponding condition, the wetting front in preferential flow domain is much faster than that in matrix domain, which causes the non-equilibrium phenomenon in terms of different water contents and pressure heads between two domains. The pressure difference between two domains drives the water exchange fluxes. The simulated results obtained by our Python code showed good agreement with the HYDRUS-1D simulations.

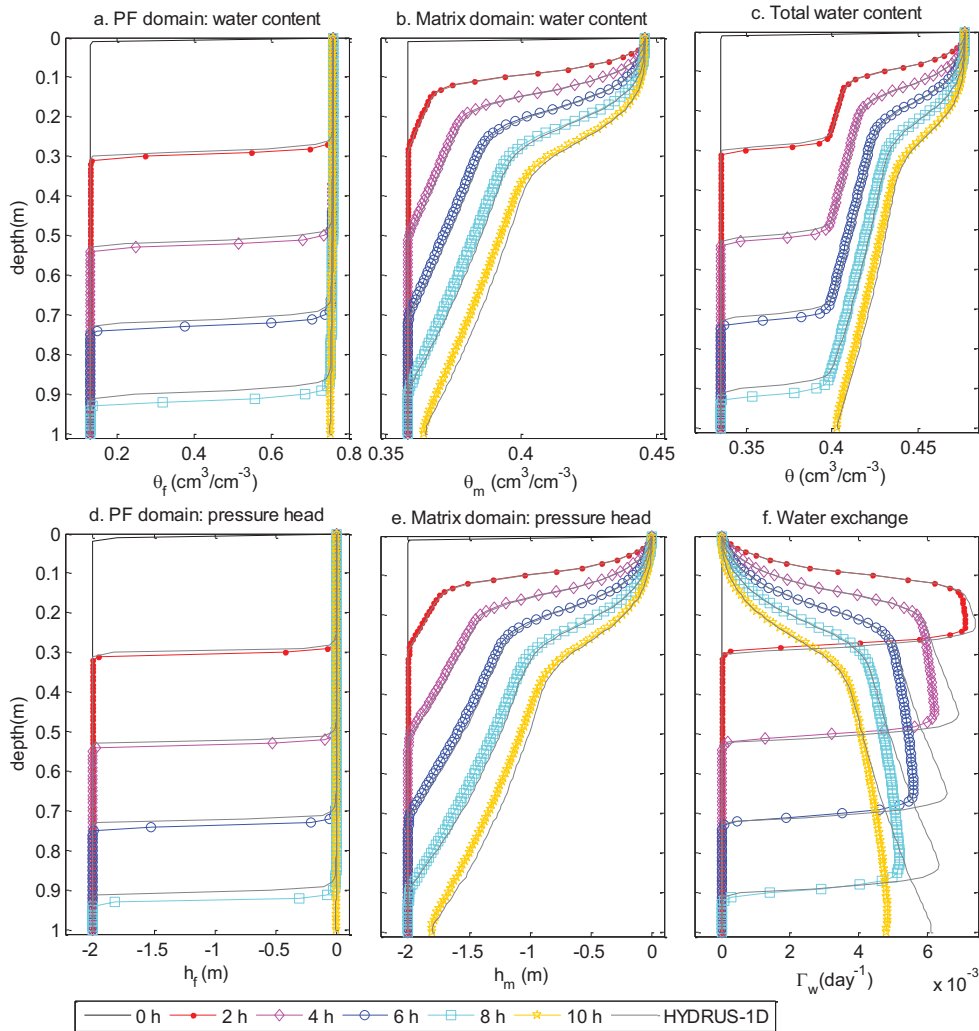


Fig 2. Benchmark the simulated hydrology results under ponding infiltration with HYDRUS-1D

4. Example of combined hillslope hydrology and soil mechanics analysis

In this section we present the results of combined hillslope hydrology and slope stability analysis for a synthetic slope that has dual-permeability hydraulic features. We used a 100m long slope with 1.5 m thick clay soil overlying an impermeable bedrock, and the slope angle is set to 30°. Table 2 shows the soil hydraulic parameters²⁴. Furthermore, we specify the soil mechanical parameters as follows: the dry bulk density is 1.62 kg/m³, the friction angle is 25°, and the effective cohesion is 6 kPa. For specifying the initial condition, the water storage variation is neglected. Thus, the initial groundwater table of the hillslope is influenced by lateral drainage, which is mainly controlled by topography (slope angle and thickness), soil hydraulic properties (hydraulic conductivity), and long-term meteorological conditions (rainfall and evaporation). For instance, if we consider a net rainfall of 1000 mm/year, the initial groundwater table estimated with Equation (1) is approximately 54 cm above the bedrock. Hereafter, the initial pressure distribution in two domains can be specified as the steady state pressure profiles following Equation (4). In our simple synthetic experiment, the rainfall event is set as a constant 10 mm/h with a duration of 10 hours (Fig.3a), and such a rainfall is sufficient to induce transient pressure response and landslide in the defined hillslope.

Table 2 Soil hydraulic parameters for the dual-permeability model in Experiment 2

Sandy loam (depth:1.5 m)	w	$\theta_l(\text{cm}^3/\text{cm}^3)$	$\theta_g(\text{cm}^3/\text{cm}^3)$	$K_s(\text{cm}/\text{day})$	$a_{VG}(\text{cm}^{-1})$	n_{VG}	l_{VG}	$\alpha_w(\text{cm}^{-2})$
Matrix domain	0.9	0.05	0.35	2.01	0.01	2.5	0.5	0.006
Preferential flow domain	0.1	0.0	0.60	1000	0.10	1.2	0.5	

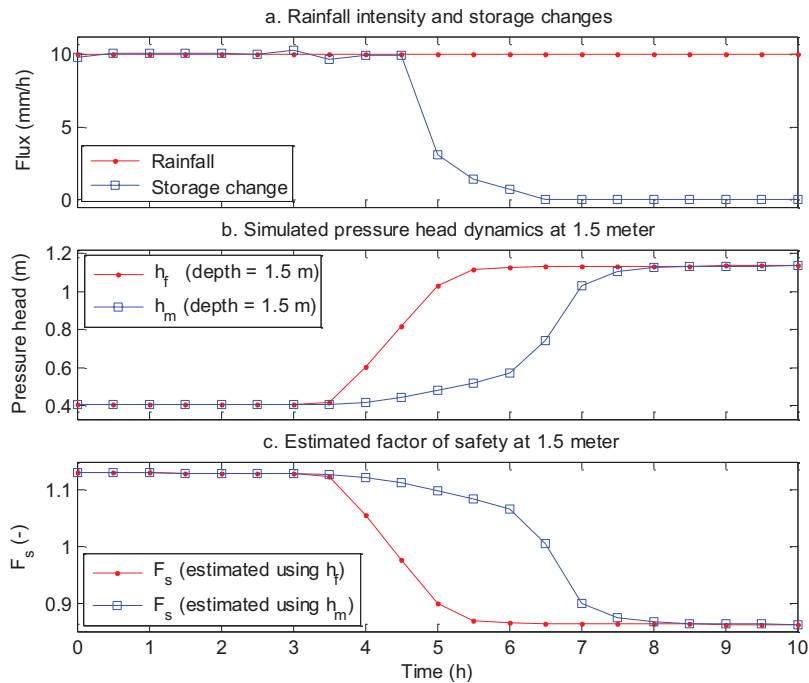


Fig.3 The simulated soil storage, pressure head and factor of safety under Experiment 2 with a 10 mm/h rainfall

The simulated water storage changes, and pressure head at 1.5 m depth of the two domains are given in Fig.3. The mass-balance error is less than 2% during the first 5 hours, after which the soil profile is approaching full-saturation and the storage variation is approaching zero (Fig. 3a). The dual-permeability model simulates pressure heads for both domains (Fig.3b). In Figure 3c we provide the calculated factor of safety using either h_f or h_m to demonstrate the influence on slope stability of the selection of the pore water pressure information: from the matrix or from the preferential flow domain. The factor of safety calculated with h_f shows a 2-hour earlier failure time than that calculated with h_m (Fig.3c).

Figure 4 shows the detailed hydrological results of the numerical simulations. In case the rainfall intensity is larger than the infiltration capacity of the matrix domain, surface ponding develops (positive pressure head, Fig. 4 b,e) and a clear saturated wetting front in the matrix domain. However, the rainfall intensity is not sufficient to cause a surface ponding on the preferential flow domain. The wetting front in the preferential flow domain remains unsaturated, and consequently the pressure head in preferential flow domain is lower than that in matrix domain (Fig. 4a, d). Therefore, water exchange occurs from the matrix towards preferential flow domain in the shallow surface soil (0-10 cm) (Fig. 4f).

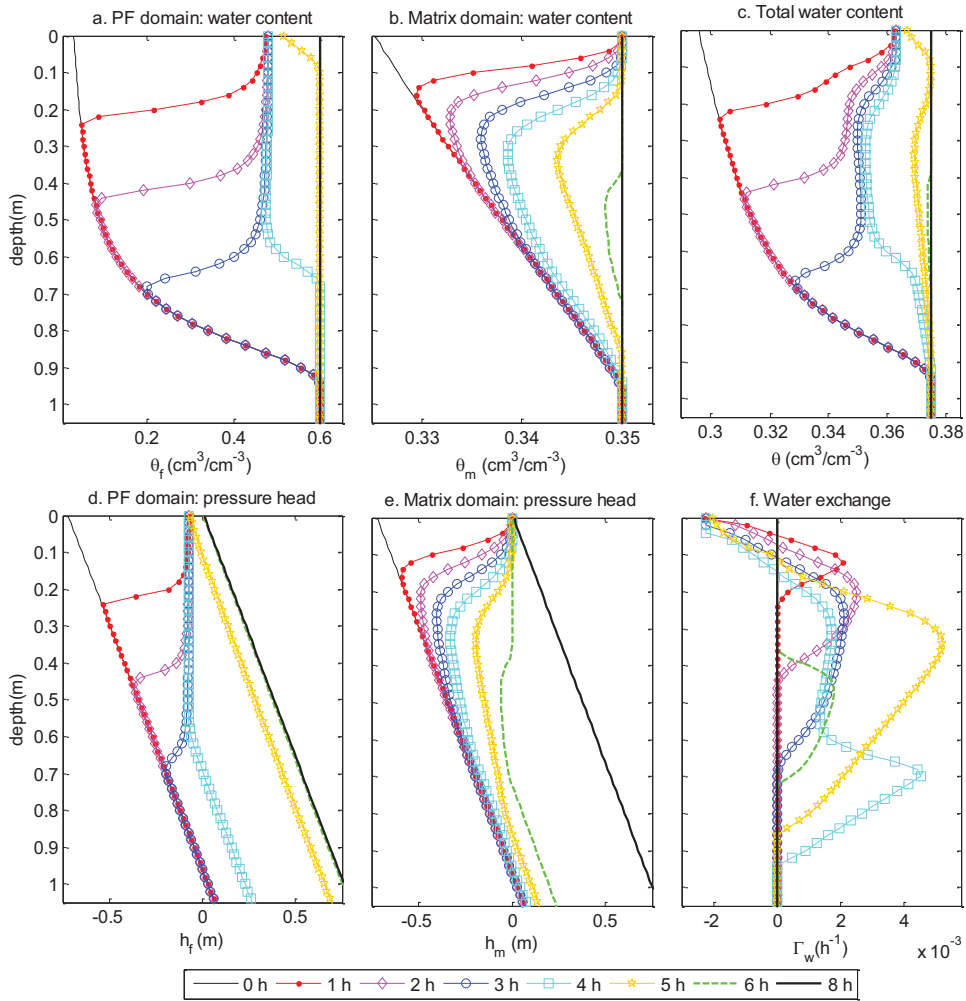


Fig. 4 The simulated soil hydrology profiles under Experiment 2 with a 10 mm/h rainfall

However, as the wetting front (unsaturated) progressed faster in the preferential flow domain, water exchange takes place from preferential domain towards matrix domain (Fig.4f) and furthermore, water reaches the lowest part of the soil matrix via preferential flow path, so by-passing the soil matrix. The pressure response in preferential flow is much quicker than that in matrix domain, and the preferential flow develops a perched groundwater table after sufficient amount (36 mm) of rainfall. Consequently, the pressure head of preferential flow in deeper soil is larger than that of matrix flow domain, which drives a positive water exchange flow transferring water from the preferential flow domain to the matrix domain (Fig.4f: 4-6 h). Finally, the pressure head of the two domains will reach an equilibrium condition after 8 hours (Fig.4 d, e).

5. Conclusions

This study presented a 1D hydro-mechanical model that integrated a modified dual-permeability model with infinite slope stability approach, which can quantify the influence of preferential flow on pressure propagation and slope failure initiation under different slope angles in a fast and relatively simple way. The model was tested with two

numerical examples. The first experiment benchmarked the newly-developed model against the HYDRUS-1D software, and showed that the author-programmed Python code provides a reliable and fast numerical solution to simulate the combined matrix flow and preferential flow as well as the complex subsurface flow processes. Secondly, we report on a synthetic numerical experiment for combined hillslope hydrology and soil mechanics analyses, which highlighted the complex soil hydrological conditions which control water and pressure wave propagations in the case of a dual-permeability subsurface. The proposed model is a relatively simple and useful tool for coupling the dual-permeability model and slope stability analysis. The planned future work includes the extension of the dual-permeability model to simulate complex natural hydrological systems under the influence of evaporation, transpiration, interception, surface runoff, etc.

References

1. Westen CJ, T W J Asch, and R Soeters. Landslide hazard and risk zonation—why is it still so difficult?. *Bull Eng Geol Environ* 2006;**65**(2):167-184.
2. Guzzetti F, A Carrara, M Cardinali, and P Reichenbach. Landslide hazard evaluation: a review of current techniques and their application in a multi-scale study, Central Italy. *Geomorphology* 1999;**31**(1–4): 181-216.
3. Rosso R, M C Rulli, and G Vannucchi. A physically based model for the hydrologic control on shallow landsliding. *Water Resources Research* 2006;**42**(6): W06410.
4. Ng C, and Y Pan. Influence of Stress State on Soil-Water Characteristics and Slope Stability. *Journal of Geotechnical and Geoenvironmental Engineering* 2000;**126**(2): 157-166.
5. Iverson R M. Landslide triggering by rain infiltration. *Water Resources Research* 2000;**36**(7): 1897-1910.
6. Berti M, and A Simoni. Field evidence of pore pressure diffusion in clayey soils prone to landsliding. *Journal of Geophysical Research: Earth Surface* 2010;**115**(F3): F03031.
7. Uchida, T., K. i. Kosugi, and T. Mizuyama. Effects of pipeflow on hydrological process and its relation to landslide: a review of pipeflow studies in forested headwater catchments. *Hydrological Processes* 2001;**15**(11): 2151-2174.
8. Hencher S R. Preferential flow paths through soil and rock and their association with landslides. *Hydrological Processes* 2010;**24**(12): 1610-1630.
9. Sidle R C, S Noguchi, Y Tsuboyama, and K Laursen. A conceptual model of preferential flow systems in forested hillslopes: evidence of self-organization. *Hydrological Processes* 2001;**15**(10): 1675-1692.
10. Nieber J L, and R C Sidle. How do disconnected macropores in sloping soils facilitate preferential flow?. *Hydrological Processes* 2010;**24**(12): 1582-1594.
11. Krzeminska D, T Bogaard, J-P Malet, and L van Beek. A model of hydrological and mechanical feedbacks of preferential fissure flow in a slow-moving landslide. *Hydrology and Earth System Sciences* 2013;**17**(3): 947-959.
12. Jarvis N J, A review of non-equilibrium water flow and solute transport in soil macropores: principles, controlling factors and consequences for water quality. *European Journal of Soil Science* 2007;**58**(3): 523-546.
13. Köhne J M, S Köhne, and J Šimůnek. A review of model applications for structured soils: a) Water flow and tracer transport. *Journal of Contaminant Hydrology* 2009;**104**(1–4):4-35.
14. Šimůnek J, N J Jarvis, M T van Genuchten, and A Gärdenäs. Review and comparison of models for describing non-equilibrium and preferential flow and transport in the vadose zone. *Journal of Hydrology* 2003;**272**(1–4):14-35.
15. Gerke H H, and M T van Genuchten. Evaluation of a first-order water transfer term for variably saturated dual-porosity flow models. *Water Resources Research* 1993; **29**(4): 1225-1238.
16. Shao W, T A Bogaard, M Bakker, and R Greco. Quantification of the influence of preferential flow on slope stability using a numerical modelling approach. *Hydrol Earth Syst Sci* 2015;**19**(5): 2197-2212.
17. Shao W, T Bogaard, and M Bakker. How to Use COMSOL Multiphysics for Coupled Dual-permeability Hydrological and Slope Stability Modeling. *Procedia Earth and Planetary Science* 2014;**9**:83-90.
18. Beven K, and P German. Macropores and water flow in soils revisited. *Water Resources Research* 2013;**49**(6):3071-3092.
19. Baum RL, J W Godt, and W Z Savage. Estimating the timing and location of shallow rainfall-induced landslides using a model for transient, unsaturated infiltration. *Journal of Geophysical Research* 2010; **115**(F3): F03013.
20. Van Genuchten M T. A closed-form equation for predicting the hydraulic conductivity of unsaturated soils. *Soil Science Society of America Journal* 1980;**44**(5): 892-898.
21. Lu N, and J Godt. Infinite slope stability under steady unsaturated seepage conditions. *Water Resources Research* 2008, **44**(11): W11404.
22. Lu N, J W Godt, and D T Wu. A closed-form equation for effective stress in unsaturated soil. *Water Resources Research* 2010, **46**(5), W05515.
23. Šimůnek J, Šejna M, Saito H, et al. The HYDRUS-1D software package for simulating the movement of water, heat, and multiple solutes in variably saturated media, version 4.0, HYDRUS software series 3. Department of Environmental Sciences, University of California Riverside, Riverside, California, USA, 2008: 315.
24. Köhne J M, S Köhne, and H. H. Gerke. Estimating the hydraulic functions of dual-permeability models from bulk soil data. *Water Resources Research* 2012;**38**(7):26-21.
25. Bogaard T, Analysis of hydrological processes in unstable clayey slopes. *Dissertation, Universiteit Utrecht, Utrecht*; 2001.